Pakistan Veterinary Journal

ISSN: 0253-8318 (PRINT), 2074-7764 (ONLINE)
DOI: 10.29261/pakvetj/2026.022

RESEARCH ARTICLE

Decoding Metabolic Reprogramming-Related Genes in Porcine Liver Development: Temporal Dynamics from Embryogenesis to Postnatal Maturation

Xiaofeng Li[1], Bo Zhang[2*] and Bing Yang[1,2,3*]

[1]College of Animal Science and Technology, Ningxia University, Yinchuan 750021, China; [2]State Key Laboratory of Animal Biotech breeding, College of Animal Science and Technology, China Agricultural University, Beijing 100193, China; [3]College of Animal Science, Anhui Science and Technology University, Fengyang 233100, China
*Corresponding author: bingyang19860919@163.com (BY); bozhang0606@cau.edu.cn (BZ)

ARTICLE HISTORY (25-541)

Received: June 10, 2025
Revised: January 06, 2026
Accepted: January 20, 2026
Published online: February 10, 2026

Key words:
Liver
Metabolic reprogramming
Porcine
Postnatal maturation

A B S T R A C T

The objective of this research was to explore the regulatory functions of metabolic reprogramming-related genes on the development of porcine liver during embryonic growth and postnatal maturation. Hepatic specimens were collected at fetal (94 days post-conception, dpc) and postnatal (1, 28, and 188 days postnatum, dpn) stages for transcriptomic analysis. We used an integrated bioinformatics method, which included differential expression analysis, multi-database pathway enrichment, and protein-protein interaction network analysis, to find and rank important genes. Metabolism-related genes were curated from GeneCards. Comparing the transcriptomes showed an increase in genomic activation over time, with differentially expressed gene (DEG) patterns depending on the stage:1,939 (1dpn vs. 94dpc), 1,448 (28 vs. 1dpn), and 880 DEGs (188 vs. 28dpn). Cross-stage analysis identified 182 conserved DEGs, among which 67 were metabolic reprogramming-related genes. Functional annotation indicated that there were enrichments of the development process (cell differentiation, mitotic spindle organization) and metabolism process (PI3K-Akt signaling pathway, fatty acid degradation, and focal adhesion). Network topology analysis revealed 9 hub genes (such as *VCL*, *CCNB1*, *HSP90AA1*) that may control hepatic maturation. In short, it demonstrates how metabolism changes over time during pig liver formation. Conserved metabolic regulators such as *LMNB1* and *CAV1* are found to be important coordinators of hepatic differentiation and metabolic adaptation. The findings provide a clear picture of the transcriptional path leading to metabolic reprogramming at various stages of pig liver development.

To Cite This Article: Li X, Zhang B and Yang B, 2026. Decoding metabolic reprogramming-related genes in porcine liver development: temporal dynamics from embryogenesis to postnatal maturation. Pak Vet J, 46(2): 282-298. http://dx.doi.org/10.29261/pakvetj/2026.022

INTRODUCTION

The liver acts as a central metabolic hub to control the metabolism of nutrients, detoxification, and maintain homeostasis of the whole body in mammals (Qian *et al.*, 2021). Porcine hepatic development has undergone important changes at two times: Embryogenesis, when the piglet is growing inside its mom, and postnatal maturation when it's born. Changes that happen during these times affect three big things: how well something grows, being able to use different kinds of food for energy and fighting off sicknesses. All of these are important for farms and doctors (Rao *et al.*, 2023; Shastak & Pelletier, 2024; Ruggeri *et al.*, 2025). And also, swine hepatogenesis keeps some of the same regulations as humans, so it's a good way to test organ creation and problems with using energy in the body. Embryonic stages (such as 94 days post-conception, dpc) create hepatic primordia and functional zonation, whereas postnatal maturation (such as 1-28 days postnatally, dpn) fosters cell differentiation and metabolic specialization to satisfy rising physiological needs (Rao et *al.*, 2023; Shastak & Pelletier, 2024; Ruggeri *et al.*, 2025). These changes can cause someone's metabolism to stay broken forever, so we need to find out why a pig's liver grows properly.

Metabolic reprogramming refers to some changes in the energy of cells, it can control the growth, differentiation, and function of hepatocytes when the liver is formed (Slabber & Tchorz, 2025; Li *et al.*, 2025). Balances energy homeostasis and biosynthetic needs,

particularly during crucial periods such as birth and weaning (Nakagaki *et al.*, 2018; Zhou *et al.*, 2024). PI3K-Akt signaling, focal adhesion dynamics, and fatty acid oxidation are central pathways implicated in hepatic metabolic shifts (Li *et al.*, 2022). But the time of metabolic reprogramming related genes and their hierarchical interactomes is still unknown for swine. Rodents and humans show that *CAV1* (lipid metabolism modulation) and *LMNB1* (mitotic nuclear organization) have conserved roles in hepatogenesis (Kokkinakis *et al.*, 2005; Ma *et al.*, 2021), but species-specific regulatory differences need separate studies on pigs. *CCNB1* controls the cell cycle during hepatocyte growth (Tian *et al.*, 2022), and *ACADVL* regulates mitochondrial β-oxidation, which is the primary source of energy in postnatal livers (Zhang *et al*., 2020). HSD17B2 and VCL have similar functions to maintain hepatic energy balance by regulating gluconeogenesis and focal adhesion remodeling during stellate cell maturation (Kawai *et al.*, 2003; Khristi *et al.*, 2019).

This research supplies a spatiotemporal regulatory system of metabolic reprogramming-related genes in porcine liver growth from the embryonic period (94dpc) to postnatal maturation (188dpn). Combine multi-stage transcriptomics with computational biology, such as differential expression analysis, multi-ontology pathway enrichment, and network-based prioritization, to find out the stage-specific regulators of metabolic adaptation. It helps us know better how pig livers change what they do with food, and it gives us ideas about making animals healthier and comparing human livers that are getting bigger and having trouble using food.

MATERIALS AND METHODS

Ethical statement: Animal care and tissue collection were carried out according to the rules set by the German Law on the Protection of Animals and had the approval of the Animal Care Committee of Mecklenburg-Vorpommern (LVLMV/TSD/7221.3-1.1-006/04).

Experimental design and tissue sampling: In 2012, Oster et al. carried out a study on 21 first-time pregnant German Landrace sows that were given a 12.1% protein diet (with a protein-to-carbohydrate ratio of 1:5) throughout their pregnancy. Liver samples were taken from the offspring of four different development stages randomly chosen, including gestational day 94 (dpc), postnatal days 1, 28, and 188 (dpn), and there were six biological replicates for each stage. Sex ratio of offspring at every stage was kept at 1:1. Prenatal sampling was done with Caesarean section of three sows per dietary group at 94 dpc, giving eight viable fetuses per so that were systematically collected from uterine horns. After euthanasia with T61 intravenous injection, about 500mg of liver samples were immediately frozen in liquid nitrogen and stored at -80°C. All the sampled litter had at least 11 live fetuses. Postnatal specimens were obtained from prostaglandin-induced parturitions (mean gestation 115 days), choosing six sows per diet group having at least 11 live births (median litter size 13). Neonates were categorized into groups at 1, 28, and 188 dpn. Extreme-weight piglets per litter were euthanized with a combination of Combelen (0.2mL) and Ursotamin (50mg) at 36hours postpartum, and the liver tissues were treated similarly to the prenatal samples. The remaining piglets were cross-fostered to multiparous sows and raised under standard conditions with free access to age-appropriate diets.

RNA processing and microarray analysis: For the microarray analysis, we chose six gender-balanced sibling pairs for each developmental stage; the first day post-natal (1dpn) had extreme birth weights, whereas other stages had random weights. Total RNA was extracted with Tri-Reagent (Sigma-Aldrich), then treated with DNase and purified using RNeasy Mini Kit (Qiagen). RNA quality was checked by agarose gel electrophoresis and NanoDrop ND1000 spectrophotometer. DNA-free preparations were checked by GAPDH-specific PCR. Biotin-labeled cDNA was generated through the use of the GeneChip 3' Express Kit (Affymetrix) and then fragmented before being hybridized onto Affymetrix Porcine Genome Arrays. After hybridization, the standard staining/washing procedure was carried out, and then the arrays were scanned on Affymetrix equipment. All experiments were performed according to the guidelines for animal welfare by the institution and carried out at the FBN experimental station.

Microarray data and metabolic reprogramming-related genes acquisition: Gene expression microarray dataset GSE33740 was obtained from the GEO database (https://www.ncbi.nlm.nih.gov/geo/). Created by the Affymetrix pig Genome Array, this data consists of liver samples from four development stages: 94dpc (n=6; GSM833868-873), 1dpn (n=6; GSM833874-879), 28dpn (n=6; GSM833880-885), and 188dpn (n=4; GSM833886-889). We utilized the GeneCards database (https://www.genecards.org/) to search for "metabolic reprogramming" and used a filter to identify protein-coding genes to obtain the required gene set.

Differential gene expression analysis: Differential expression analysis was carried out by means of the GEO2R tool (http://www.ncbi.nlm.nih.gov/geo/geo2r) with default settings that include quantile normalization and comparison of gene expression profiles among liver samples at certain time points. GEO2R uses the Limma package in R, which is designed for analyzing microarray data. Genes with $|\log_2 FC| \geq 1.00$ and $P<0.05$ were considered as DEGs. Overlapping DEGs from consecutive time point comparisons (1dpn vs. 94dpc, 28 vs. 1dpn, and 188 vs. 28dpn) were determined for additional investigation, excluding those without Entrez gene annotations. P-value adjustments were made using the Benjamini-Hochberg false discovery rate method to account for multiple tests.

Functional enrichment analysis: To find out what those DEGs do biologically, we did a GO enrichment analysis on them with the help of the DAVID database (https://david.ncifcrf.gov/summary.jsp). And also, we have done the functional enrichment analysis with KEGG, Reactome, and PANTHER pathways via the KOBAS 3.0 database (http://kobas.cbi.pku.edu.cn/kobas3/genelist/). Proteins encoded by the DEGs were classified based on their protein sequences using the PANTHER database (http://pantherdb.org/tools/compareToRefList.jsp).

Protein-protein interaction networks: Construct PPI network based on DEGs from pairwise comparison at certain time points (1dpn vs. 94dpc, 28 vs. 1dpn, and 188 vs. 28dpn). The construct process was carried out through the use of STRING software (https://string-db.org/). This software is well-known for predicting protein interactions. Then, these PPI networks were drawn by Cytoscape software (version 3.8.0; http://www.cytoscape.org/). Cytoscape gives good ways to see and check complicated networks, so scientists can know how different DEGs work together.

Hub genes and their functions: Hub genes that serve as critical nodes within the PPI network were identified through various algorithms available within the CytoHubba plugin of Cytoscape. The specific algorithms used were: Maximal Clique Centrality, Edge Percolated Component, Maximum Neighborhood Component, Closeness Centrality, and Density of Maximum Neighborhood Component. These algorithms are designed to find the most important genes that have a large impact on how the network operates. Biological functions of these hub genes were analyzed according to related literature, NCBI database (https://www.ncbi.nlm.nih.gov/), and GeneCards (https://www.genecards.org/).

RESULTS

Transcriptome profiling of liver: Fig. 1A-C shows the results of UMAP dimensionality reduction, transcript expression patterns, and expression density distributions. The transcriptomic analysis on the liver tissue from four different developmental stages (94dpc, 1dpn, 28dpn, and 188dpn) has found 6,289-6,313 unique genes. Differential gene expression profiles of pairwise comparison (1dpn vs. 94dpc, 28 vs. 1dpn, 188 vs. 28dpn) were illustrated by volcano plots in Figs. 1D-F. To find out the genes that have a dynamic expression trajectory, we make a Venn diagram to show the overlapping DEGs among the three comparisons (Fig. 1G).

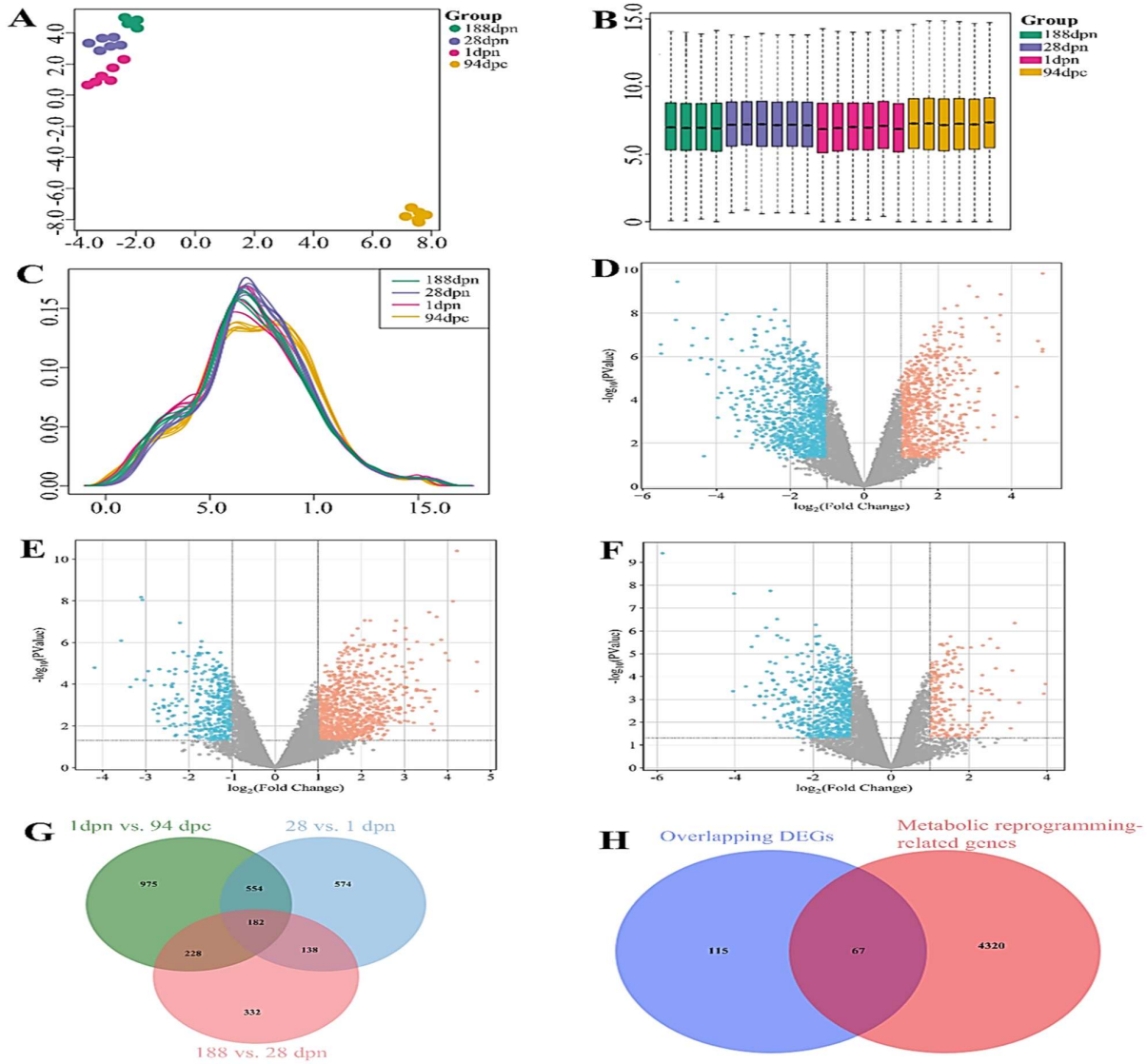

Fig. 1 Transcriptomic landscape of porcine liver development. (A-C) indicate UMAP, transcript expression, and expression density, respectively. (D-F) represent the volcano plots for the three comparisons of 1dpn vs. 94dpc, 28 vs. 1dpn, and 188 vs. 28dpn, respectively. The red and blue points reveal the up-and down-regulated genes, and the gray spots mean the unchanged genes. (D) reveals the Venn diagram for the DEGs from the three comparisons. (H) indicates the Venn diagram for metabolic reprogramming-related DEGs.

Pairwise comparison showed that there was considerable transcriptional reprogramming occurring during hepatic maturation, with 880-1,939 DEGs identified at each transition in development (Table 1). In contrast to 94dpc, 1dpn had 792 up-regulated and 1,147 down-regulated genes. Compared to 1dpn, 28dpn has 1,027 up-regulated and 421 down-regulated genes (Table 1). 188 vs. 28dpn comparison has 212 upregulated and 668 downregulated genes (Table 1). Also, a core group of 182 overlapping DEGs among all comparisons was found, which indicates genes with constant expression alterations.

To distinguish important transcriptional regulators during late embryogenesis and postnatal development, we have thoroughly examined the most dramatically altered genes throughout various stages of growth. In our analysis, we have found the top 20 up-regulated and down-regulated genes for each sequential stage (1dpn vs. 94dpc, 28 vs. 1dpn, 188 vs. 28dpn; Table 2-7). We have also discovered 67 metabolic reprogramming-related DEGs (Table 8 and Fig. 1H), which show that there are some key energy adaptation pathways. Finally, it provides an overall picture of how hepatocytes differentiate by identifying stage-specific regulators and persistent metabolic signatures.

GO enrichment of DEGS: DAVID was applied for GO enrichment analysis of DEGs at various stages of porcine liver growth. From the result, we can observe that most of the DEGs between 1dpn and 94dpc are related to the beginning of the development process (Fig. 2A). Then the 28 vs 1dpn comparison suggests transitional adaptations involving intracellular trafficking and glucose homeostasis (Fig. 2B). Late maturation, 188 vs. 28dpn comparison has to do with tissue remodelling and better energy metabolism (Fig. 2C). The most remarkable finding is that out of the 182 conserved DEGs found through cross-comparison analysis, these genes have a considerable connection to cytoskeleton rearrangement and nuclear-cytoplasmic transportation (Fig. 2D).

Table 1: The DEGs identified in the porcine liver

Items	Total	Up-regulated	Down-regulated
1dpn vs 94dpc	1,939	792	1,147
28dpn vs 1dpn	1,448	1027	421
188dpn vs 28dpn	880	212	668

Table 2: Top 20 upregulated genes in the liver of pig at 1dpn compared with that at 94dpc

Gene symbol	Expression (log_2FC)	Up- or down-regulated	*P* Value	Description
PDK4	4.84	Upregulated	4.53E-07	Pyruvate dehydrogenase kinase 4
CKMT2	4.84	Upregulated	1.46E-10	Creatine kinase, mitochondrial 2 (sarcomeric)
ATP5I	4.83	Upregulated	5.89E-07	ATP synthase, H+ transporting, mitochondrial Fo complex, subunit E
TP53INP2	4.71	Upregulated	1.92E-07	Tumor protein p53 inducible nuclear protein 2
CST6	4.14	Upregulated	2.49E-05	Cystatin E/M
COMT	4.13	Upregulated	6.28E-04	Catechol-O-methyltransferase
HSPB7	3.70	Upregulated	1.36E-09	Heat shock 27kda protein family, member 7
FKBP5	3.69	Upregulated	1.21E-08	FK506 binding protein 5
MYO5B	3.65	Upregulated	1.87E-07	Myosin VB
TRNP1	3.65	Upregulated	9.24E-08	TMF1-regulated nuclear protein 1
TRIP10	3.61	Upregulated	5.60E-06	Thyroid hormone receptor interactor 10
AGT	3.58	Upregulated	5.96E-06	Angiotensinogen
PELI1	3.51	Upregulated	5.05E-04	Pellino E3 ubiquitin protein ligase 1
SRSF10	3.50	Upregulated	1.82E-03	Serine/arginine-rich splicing factor 10
DDO	3.48	Upregulated	4.36E-08	D-aspartate oxidase
ATP2A1	3.31	Upregulated	1.63E-08	Atpase, Ca^{2+} transporting, cardiac muscle, fast twitch 1
TAF1D	3.28	Upregulated	6.98E-03	TATA-box binding protein associated factor, RNA polymerase I subunit D
ANKRD2	3.12	Upregulated	3.01E-05	Ankyrin repeat domain 2
COX10	3.11	Upregulated	4.12E-05	COX10 homolog, cytochrome c oxidase assembly protein, heme A
ANGPTL4	3.10	Upregulated	1.19E-04	Angiopoietin-like 4

Table 3: Top 20 downregulated genes in the liver of pig at 1dpn compared with that at 94dpc

Gene symbol	Expression (log_2FC)	Up- or down-regulated	*P* Value	Description
TNNT2	-5.51	downregulated	2.76E-07	Troponin T type 2
SLC31A2	-5.50	downregulated	7.26E-07	Solute carrier family 31 member 2
MDK	-5.10	downregulated	2.05E-08	Midkine (neurite growth-promoting factor 2)
MYL4	-5.06	downregulated	3.48E-10	Myosin, light chain 4, alkali; atrial, embryonic
THY1	-4.72	downregulated	1.45E-06	Thy-1 cell surface antigen
FSCN1	-4.66	downregulated	3.06E-07	Fascin actin-bundling protein 1
DCLK1	-4.63	downregulated	4.81E-08	Doublecortin-like kinase 1
IGSF1	-4.42	downregulated	1.16E-06	Immunoglobulin superfamily, member 1
ORM1	-4.34	downregulated	3.96E-02	Orosomucoid 1
POSTN	-4.26	downregulated	1.42E-07	Periostin, osteoblast specific factor
SPOCK3	-4.24	downregulated	6.52E-06	Sparc/osteonectin, cwcv and kazal-like domains proteoglycan 3
C8H4orf48	-4.14	downregulated	1.34E-06	Chromosome 8 open reading frame, human c4orf48
PRKRA	-3.96	downregulated	6.63E-04	Protein activator of interferon induced protein kinase EIF2AK2
SKA1	-3.96	downregulated	8.04E-05	Spindle and kinetochore associated complex subunit 1
RASGEF1A	-3.92	downregulated	3.13E-06	Rasgef domain family, member 1A
C3H2orf40	-3.87	downregulated	4.79E-05	Chromosome 3 open reading frame, human c2orf40
ITGA2	-3.84	downregulated	1.57E-06	Integrin, alpha 2
VCAN	-3.84	downregulated	2.02E-08	Versican
NUF2	-3.79	downregulated	4.40E-06	NUF2, NDC80 kinetochore complex component
BCAR3	-3.73	downregulated	1.12E-08	Breast cancer anti-estrogen resistance 3

Table 4: Top 20 upregulated genes in the liver of pig at 28dpn compared with that at 1dpn

Gene symbol	Expression (log_2FC)	Up- or down-regulated	*P* Value	Description
CYP3A29	4.68	Upregulated	8.36E-06	Cytochrome P450 3A29
PRKRA	4.68	Upregulated	2.13E-04	Protein activator of interferon induced protein kinase EIF2AK2
PYGM	4.22	Upregulated	4.01E-11	Phosphorylase, glycogen, muscle
GAMT	4.12	Upregulated	1.04E-08	Guanidinoacetate N-methyltransferase
SNTB1	4.02	Upregulated	7.14E-06	Syntrophin beta 1
CYP27A1	3.95	Upregulated	3.15E-06	Cytochrome P450, family 27, subfamily A, polypeptide 1
KYAT1	3.85	Upregulated	7.28E-07	Kynurenine aminotransferase 1
MSS51	3.74	Upregulated	5.82E-08	MSS51 mitochondrial translational activator
UBE3D	3.73	Upregulated	1.92E-03	Ubiquitin protein ligase E3D
CDKN1B	3.69	Upregulated	1.76E-04	Cyclin-dependent kinase inhibitor 1B
SLPI	3.68	Upregulated	1.58E-02	Secretory leukocyte peptidase inhibitor
PLBD1	3.64	Upregulated	1.23E-06	Phospholipase B domain containing 1
DEDD	3.63	Upregulated	7.97E-03	Death effector domain containing
CCL5	3.58	Upregulated	4.61E-04	Chemokine (C-C motif) ligand 5
MAPKAP1	3.58	Upregulated	6.88E-04	Mitogen-activated protein kinase associated protein 1
BCAR3	3.57	Upregulated	3.50E-08	Breast cancer anti-estrogen resistance 3
KCNIP2	3.50	Upregulated	4.46E-04	Kv channel interacting protein 2
GPD1	3.49	Upregulated	2.13E-04	Glycerol-3-phosphate dehydrogenase 1
NCALD	3.41	Upregulated	1.24E-03	Neurocalcin delta
NR3C1	3.41	Upregulated	1.99E-04	Nuclear receptor subfamily 3, group C, member 1

Table 5: Top 20 downregulated genes in the liver of pig at 28dpn compared with that at 1dpn

Gene symbol	Expression (log_2FC)	Up- or down-regulated	*P* Value	Description
GALT	-4.19	downregulated	1.59E-05	Galactose-1-phosphate uridylyltransferase
KLK1	-3.57	downregulated	8.06E-07	Kallikrein 1
MYO5B	-3.36	downregulated	1.35E-04	Myosin VB
ANKRD2	-3.21	downregulated	5.84E-05	Ankyrin repeat domain 2
PEG10	-3.10	downregulated	6.59E-09	Paternally expressed 10
CDKN3	-3.07	downregulated	8.79E-09	Cyclin-dependent kinase inhibitor 3
GRAMD1B	-3.03	downregulated	6.30E-05	GRAM domain containing 1B
SHROOM3	-2.95	downregulated	2.33E-05	Shroom family member 3
NDUFA1	-2.87	downregulated	1.15E-04	NADH dehydrogenase 1 alpha subcomplex 1
ANKRD1	-2.82	downregulated	1.61E-03	Ankyrin repeat domain 1
PIPOX	-2.78	downregulated	8.65E-04	Pipecolic acid and sarcosine oxidase
RNF207	-2.71	downregulated	2.54E-03	Ring finger protein 207
UCHL1	-2.71	downregulated	5.92E-03	Ubiquitin carboxyl-terminal esterase L1
ACOT7	-2.69	downregulated	1.37E-03	Acyl-coa thioesterase 7
TRAPPC12	-2.68	downregulated	1.89E-05	Trafficking protein particle complex 12
ATP5I	-2.59	downregulated	1.07E-03	ATP synthase, H+ transporting, mitochondrial Fo complex, subunit E
DPM2	-2.59	downregulated	5.54E-04	Dolichyl-phosphate mannosyltransferase subunit 2, regulatory
WDTC1	-2.58	downregulated	1.15E-03	WD and tetratricopeptide repeats 1
GNAS	-2.57	downregulated	1.34E-03	GNAS complex locus
FOSL2	-2.56	downregulated	1.07E-04	FOS like 2, AP-1 transcription factor subunit

Table 6: Top 20 upregulated genes in the liver of pig at 188dpn compared with that at 28dpn

Gene symbol	Expression (log_2FC)	Up- or down-regulated	*P* Value	Description
UCHL1	3.96	Upregulated	2.13E-04	Ubiquitin carboxyl-terminal esterase L1
ANKRD1	3.93	Upregulated	5.64E-04	Ankyrin repeat domain 1
ETNPPL	3.29	Upregulated	1.40E-03	Ethanolamine-phosphate phospho-lyase
NANOS1	3.17	Upregulated	4.56E-07	Nanos C2HC-type zinc finger 1
TMEM140	3.11	Upregulated	5.44E-05	Transmembrane protein 140
PLA2G1B	3.07	Upregulated	1.86E-02	Phospholipase A2, group IB (pancreas)
FOS	2.78	Upregulated	1.07E-03	Fos proto-oncogene, AP-1 transcription factor subunit
ME1	2.74	Upregulated	5.60E-06	Malic enzyme 1, NADP(+)-dependent, cytosolic
MSS51	2.69	Upregulated	4.39E-05	MSS51 mitochondrial translational activator
KNG1	2.59	Upregulated	5.87E-04	Kininogen 1
PIPOX	2.59	Upregulated	6.29E-03	Pipecolic acid and sarcosine oxidase
HSP70.2	2.54	Upregulated	2.22E-06	Heat shock protein 70.2
GPX3	2.52	Upregulated	3.78E-03	Glutathione peroxidase 3
GFPT1	2.51	Upregulated	3.92E-04	Glutamine--fructose-6-phosphate transaminase 1
CLEC5A	2.43	Upregulated	4.03E-04	C-type lectin domain family 5, member A
OGFOD1	2.43	Upregulated	1.31E-02	2-oxoglutarate and iron-dependent oxygenase domain containing 1
TNFRSF12A	2.41	Upregulated	3.87E-03	TNF receptor superfamily member 12A
ARID4B	2.39	Upregulated	6.66E-03	AT rich interactive domain 4B (RBP1-like)
MYF6	2.36	Upregulated	4.32E-06	Myogenic factor 6 (herculin)
VIL1	2.36	Upregulated	1.77E-02	Villin 1

A group of 67 metabolic reprogramming related DEGs which have a two-way relationship between mitotic spindle structure and thermogenic adjustment and blood vessel formation during liver development (Fig. 2E). And also, we created heat maps to see how the overlapping DEGs that belong to calcium ions move about, normal NF-kappaB signaling pathways, cell movement, immune system response, gene amplification, cell migration improvement, natural defense reactions, moving proteins into the nucleus, and controlling cell shapes (Figs. 2F-N).

Table 7: Top 20 downregulated genes in the liver of pig at 188dpn compared with that at 28dpn

Gene symbol	Expression (log_2FC)	Up- or down-regulated	*P* Value	Description
RBP7	-5.86	downregulated	3.98E-10	Retinol binding protein 7, cellular
ACTC1	-4.05	downregulated	4.38E-04	Actin, alpha, cardiac muscle 1
ALG5	-4.02	downregulated	2.33E-08	ALG5, dolichyl-phosphate beta-glucosyltransferase
POSTN	-3.72	downregulated	2.72E-04	Periostin, osteoblast specific factor
KHNYN	-3.57	downregulated	4.98E-06	KH and NYN domain containing
LITAF	-3.50	downregulated	1.78E-03	Lipopolysaccharide induced TNF factor
DDX11	-3.43	downregulated	1.68E-06	DEAD/H-box helicase 11
FSCN1	-3.36	downregulated	7.07E-04	Fascin actin-bundling protein 1
FCN2	-3.36	downregulated	7.39E-04	Ficolin 2 (hucolin)
MYBL2	-3.34	downregulated	1.94E-04	MYB proto-oncogene like 2
TOP2A	-3.25	downregulated	6.28E-03	Topoisomerase (DNA) II alpha
GDI1	-3.24	downregulated	1.54E-03	GDP dissociation inhibitor 1
SLC38A10	-3.20	downregulated	7.37E-04	Solute carrier family 38 member 10
B2M	-3.20	downregulated	7.36E-07	Beta-2-microglobulin
MX1	-3.20	downregulated	4.19E-04	Myxovirus resistance 1, interferon-inducible protein p78
CCL21	-3.18	downregulated	6.00E-05	Chemokine (C-C motif) ligand 21
ULBP1	-3.10	downregulated	2.27E-05	UL16 binding protein 1
FNTA	-3.09	downregulated	1.76E-08	Farnesyltransferase, CAAX box, alpha
TMEM25	-3.06	downregulated	7.17E-05	Transmembrane protein 25
XAF1	-3.03	downregulated	1.40E-04	XIAP associated factor 1

KEGG pathway dynamics during hepatic maturation: To see which signaling networks control how pig liver grows, we did something called KEGG pathway enrichment analysis using KOBAS. Different pathway activation patterns occur at different stages of development: 1) Early postnatal transition (1 vs 94dpc): DEGs show activation of core metabolic regulators (PPAR, AMPK, PI3K-Akt) along with energy adaptation pathways (thermogenesis, oxidative phosphorylation, TCA cycle) and structural reorganization signals (cell adhesion molecules, Rap1) (Fig. 3A); 2) Mid-development shift (28 vs. 1dpn): Pathways have shifted toward stress-responsive networks with p53-mediated surveillance, TGF-β/TNF signaling, and precision metabolic regulation (insulin/glucagon homeostasis, amino acid catabolism) as well as quality-control mechanisms (ER protein processing, spliceosome) (Fig. 3B); 3) Late maturation phase (188 vs. 28dpn): DEGs have taken part in tissue remodeling through ECM-receptor interactions, inflammatory regulation (NF-κB, chemokine), and advanced lipid metabolism (fatty acid β-oxidation, unsaturated FA biosynthesis) (Fig. 3C).

Cross-stage conserved pathways (shared DEGs among all comparisons) showed continuous coordination for: Metabolic fine-tuning (fatty acid elongation, pyruvate / amino acid metabolism), Proliferation - Differentiation Balance (PI3K-Akt / MAPK cascade, cell cycle checkpoint), Structural Plasticity (focal adhesion, ECM interaction) (Figure 3D). Metabolic reprogramming specific DEGs formed a network connecting Rap1 cytoskeletal signaling with energy sensor pathways (AMPK/PI3K-Akt), stress-responsive regulators (p53), and branch-chain amino acid metabolism (Fig. 3E). And also, Figs. 3F-Q display the expression patterns of overlapping DEGs within signaling pathways of metabolic pathways, PI3K-Akt, MAPK, focal adhesion, valine, leucine, and isoleucine degradation, protein processing in the endoplasmic reticulum, fatty acid degradation, cell adhesion molecules, PPAR, fatty acid metabolism, cell cycle, and protein processing in the endoplasmic reticulum.

Reactome pathway enrichment analysis: As shown in Fig. 4A, the DEGs from 1dpn vs. 94dpc include metabolism, proteins metabolism, cell cycle, RNA metabolism, neutrophil degranulation, lipids metabolism, vesicle-mediated transport, M phase, TCA cycle and respiratory electron transport, cell cycle checkpoints, mitotic prometaphase, respiratory electron transport, mitotic cell cycle regulation, rRNA processing, etc. Additionally, DEGs obtained in the porcine liver between 28 and 1dpn were also found to be related to signaling pathways such as metabolism, signal transduction, protein metabolism, RNA metabolism, cell cycle, mRNA splicing, lipid metabolism, amino acid and derivative metabolism, etc. (Fig. 4B). Also, DEGs obtained from porcine liver at 188-28dpn are connected to metabolism, protein metabolism, MAPK family signaling cascades, lipid metabolism, TLR cascades, MAPK1/MAPK3 signaling, TLR4 cascade, development biology, and amino acids and derivatives metabolism, etc. (Fig. 4C).

In addition, the commonly identified DEGs among all comparisons showed enrichment for basic signaling pathways such as gene transcription, TLR cascades, cell cycle, and MAPK signaling (Fig. 4D). Especially noteworthy, the metabolic reprogramming-related DEGs were associated with key regulatory processes such as post-translational modifications, MAPK signaling, cell cycle regulation, and DNA damage responses (Fig. 4E).

Panther pathway enrichment analysis for DEGs: As shown in Fig. 5A, DEGs in porcine liver from 1dpn to 94dpc were significantly related to TCA cycle, pyruvate metabolism, TGF-beta, FAS, glycolysis, cell cycle, apoptosis, 2-arachidonoylglycerol biosynthesis, mannose metabolism, leucine biosynthesis, asparagine and aspartate biosynthesis, p53, and 5HT2 type receptor-mediated signaling pathways. Compared with 28 vs. 1dpn, DEGs are enriched for leucine biosynthesis, anandamide degradation, alanine biosynthesis, glycolysis, valine biosynthesis, JAK/STAT, FAS, isoleucine biosynthesis, Notch, T cell activation, p53, TGF-beta, 5-hydroxytryptamine biosynthesis, formyltetrahydrofolate biosynthesis, adrenaline, and noradrenaline biosynthesis (Fig. 5B).

Analysis of DEGs from 188 to 28dpn shows that they participate in pyruvate metabolism, methionine biosynthesis, p53, p38 MAPK, VEGF, 2-arachidonoylglycerol biosynthesis, B cell activation, toll receptor, formyltetrahydrofolate biosynthesis, glutamine

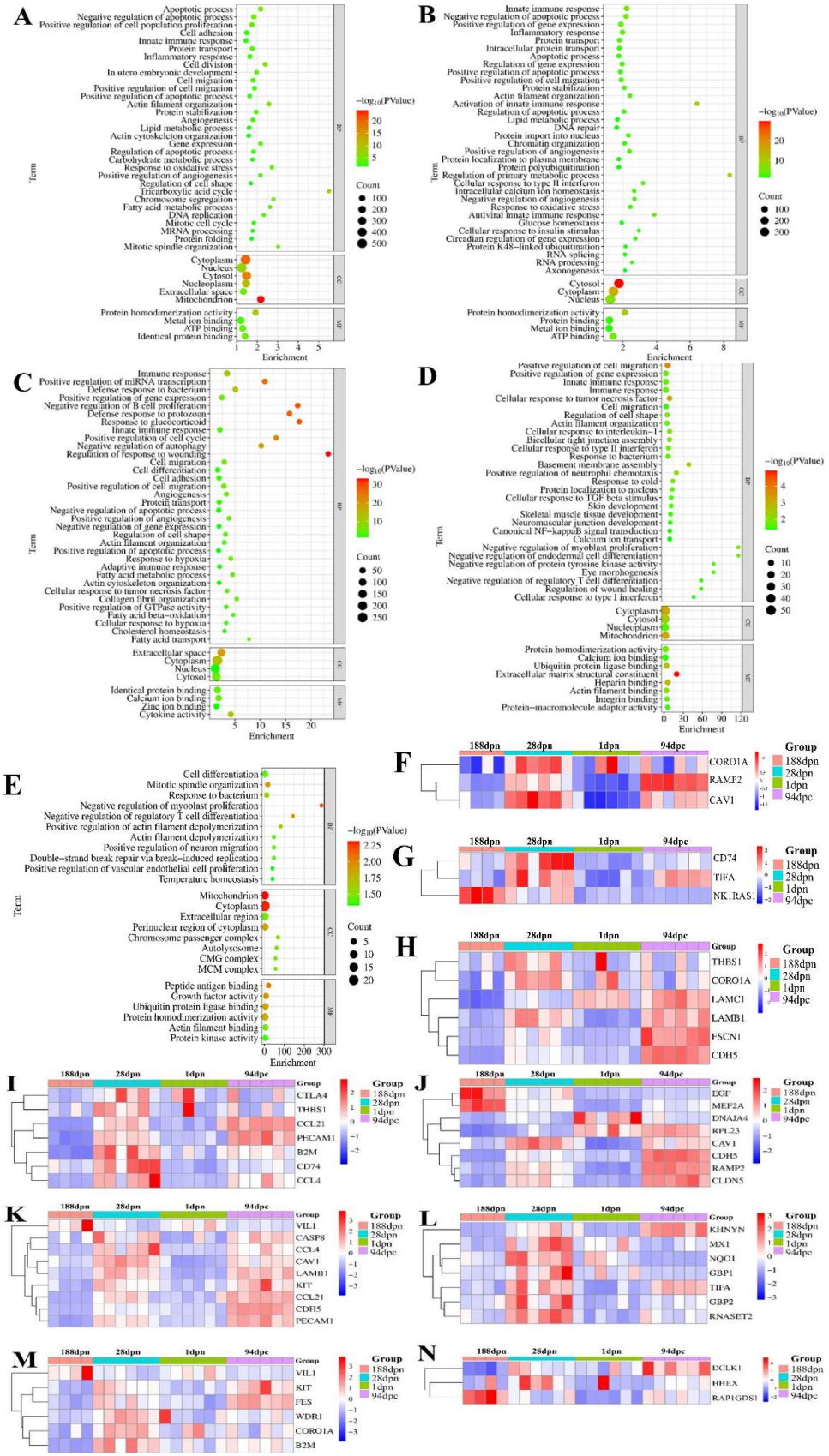

Fig. 2: GO functional annotation of the DEGs. (A-D) imply the GO enrichment for the DEGs identified in the comparison of 1dpn vs. 94dpc, 28dpn vs. 1dpn, and 188dpn vs. 28dpn, and the common DEGs in the three comparisons mentioned above. (E) highlights the GO enrichment for the metabolic reprogramming-related DEGs. (F-N) illustrate the expression profiles of the overlapping DEGs in biological processes of calcium ion transport, canonical NF-kappaB signal transduction, cell migration, immune response, positive regulation of gene expression, positive regulation of cell migration, innate immune response, protein localization to nucleus, and cell shape regulation, respectively.

Table 8: Metabolic reprogramming-associated DEGs identified in porcine liver

Gene symbol	Description
B2M	Beta-2-microglobulin
MX1	Myxovirus (influenza virus) resistance 1, interferon-inducible protein p78
ANGPTL4	Angiopoietin-like 4
CNP	2',3'-cyclic nucleotide 3' phosphodiesterase
MCM5	Minichromosome maintenance complex component 5
HHEX	Hematopoietically expressed homeobox
IGF2	Insulin-like growth factor 2
AURKB	Aurora kinase B
AURKA	Aurora kinase A
FABP3	Fatty acid binding protein 3, muscle and heart
TAP1	Transporter 1, ATP-binding cassette, sub-family B
EDC4	Enhancer of mrna decapping 4
HSDL2	Hydroxysteroid dehydrogenase like 2
CTLA4	Cytotoxic T-lymphocyte-associated protein 4
THBS1	Thrombospondin 1
TPM2	Tropomyosin 2
OVOL1	Ovo like transcriptional repressor 1
KIT	V-kit Hardy-Zuckerman 4 feline sarcoma viral oncogene homolog
ACADVL	Acyl-coa dehydrogenase, very long chain
RNASET2	Ribonuclease T2
MYOD1	Myogenic differentiation 1
VCL	Vinculin
CCNB1	Cyclin B1
NQO1	NAD(P)H dehydrogenase, quinone 1
FABP5	Fatty acid binding protein 5
ACTB	Actin, beta
CKAP4	Cytoskeleton associated protein 4
PREB	Prolactin regulatory element binding
ACAT2	Acetyl-CoA acetyltransferase 2
SHTN1	Shootin 1
GM2A	GM2 ganglioside activator
HADHB	Hydroxyacyl-coa dehydrogenase/3-ketoacyl-coa thiolase/enoyl-coa hydratase, beta subunit
PEG10	Paternally expressed 10
DCLK1	Doublecortin-like kinase 1
MDK	Midkine
WDR1	WD repeat domain 1
CAV1	Caveolin 1, caveolae protein, 22kda
MCM2	Minichromosome maintenance complex component 2
MTHFD2	Methylenetetrahydrofolate dehydrogenase 2, methenyltetrahydrofolate cyclohydrolase
ACOT9	Acyl-coa thioesterase 9
LMNB1	Lamin B1
ACOT13	Acyl-coa thioesterase 13
LAMC1	Laminin, gamma 1
IDH3B	Isocitrate dehydrogenase 3 beta
PLOD1	Procollagen-lysine, 2-oxoglutarate 5-dioxygenase 1
UBA52	Ubiquitin A-52 residue ribosomal protein fusion product 1
NDUFS3	NADH dehydrogenase Fe-S protein 3
FTL	Ferritin, light polypeptide
PTMA	Prothymosin, alpha
IVD	Isovaleryl-coa dehydrogenase
SRSF6	Serine and arginine rich splicing factor 6
HSP90AA1	Heat shock protein 90kda alpha, class A member 1
MSTN	Myostatin
PGM3	Phosphoglucomutase 3
ZFAND2A	Zinc finger AN1-type containing 2A
DEK	DEK proto-oncogene
ALDH1A1	Aldehyde dehydrogenase 1 family, member A1
MEF2A	Myocyte enhancer factor 2A
SQSTM1	Sequestosome 1
ALDH2	Aldehyde dehydrogenase 2 family
EGF	Epidermal growth factor
ETS2	ETS proto-oncogene 2, transcription factor
FKBP5	FK506 binding protein 5
KLK1	Kallikrein 1
VIL1	Villin 1
ANKRD1	Ankyrin repeat domain 1
UCHL1	Ubiquitin carboxyl-terminal esterase L1

glutamate conversion, and plasminogen activating cascade (Fig. 5C). Additionally, there are common DEGs among all three developmental stages which have been significantly related to cell cycle, integrin formyltetrahydrofolate biosynthesis, insulin/IGF/MAPK, tetrahydrofolate biosynthesis, FAS, and insulin/IGF pathway-protein kinase B signaling pathways (Fig. 5D). Metabolic reprogramming related DEGs are associated with integrin, insulin/IGF/MAP kinase cascade, p38 MAPK, formyltetrahydrofolate biosynthesis, p53 pathway, etc.

Protein classification of DEGs: Protein classifications connected to DEGs have shown changes in protein families during pectoral muscle growth. According to Figure 6A, DEGs in the porcine liver from 1dpn to 94dpc are significantly related to different kinds of protein classifications, such as pyrophosphatase, carbohydrate kinase, mutase, ligase, kinase modulator, dehydrogenase, acyltransferase, vesicle coat protein, oxidase, transfer/carrier protein, kinase activator, oxidoreductase, and chaperone. Likewise, DEGs within the pectoral muscle during the period from 28 days prior to birth to 1 day post-natal were also found to be associated with various types of proteins, such as protein-modifying enzymes, transferases, intercellular signal molecules, hydrolases, metabolite-converting enzymes, cytoskeletal proteins, RNA-metabolizing proteins, oxidoreductases, DNA-metabolizing proteins, extracellular matrix proteins, protein phosphatases, growth factors, chaperones, reductases, and RNA-processing factors (Fig. 6B).

Additionally, DEGs in the pectoral muscle from 188 to 28dpn are related to different kinds of proteins such as metabolite interconversion enzyme, oxidoreductase, transfer/carrier protein, intercellular signal molecule, growth factor, extracellular matrix protein, protease inhibitor, transferase, oxidase, acyltransferase, peroxidase, dehydrogenase, reductase, peptide hormone, galactosidase, phosphodiesterase, and cell adhesion molecule (Fig. 6C). Also noteworthy, common DEGs across the three comparisons are linked to Hsp90 family chaperone, mutase, esterase, acyltransferase, endoribonuclease, kinase activator, dehydrogenase, growth factor, extracellular matrix protein, oxidoreductase, intercellular signal molecule, and metabolite interconversion enzyme (Fig. 6D). Metabolic reprogramming-related DEGs are connected to metabolite interconversion enzyme, dehydrogenase, Hsp90 family chaperone, growth factor, mutase, oxidoreductase, esterase, chaperone, isomerase, endoribonuclease, acyltransferase, etc. (Fig. 6E).

PPI networks: To find out important regulatory genes that play a role in the growth of pig livers, we made PPI networks with the same DEGs from all three comparisons (1dpn vs. 94dpc, 28 vs. 1dpn, and 188 vs. 28dpn), along with those related to metabolism change. The obtained networks are shown in Fig. 7A-B, respectively. The network analysis of the common DEGs among the three comparisons shows some important liver development-associated genes such as *HSDL2*, *FBN1*, *CBR3*, and *FBNI*. Also, some other common DEGs are related to metabolic reprogramming, such as *HSDL2*, *HSP90AA1*, and *IVD*, which may be important regulators of liver development in pigs, as seen in Fig. 7B.

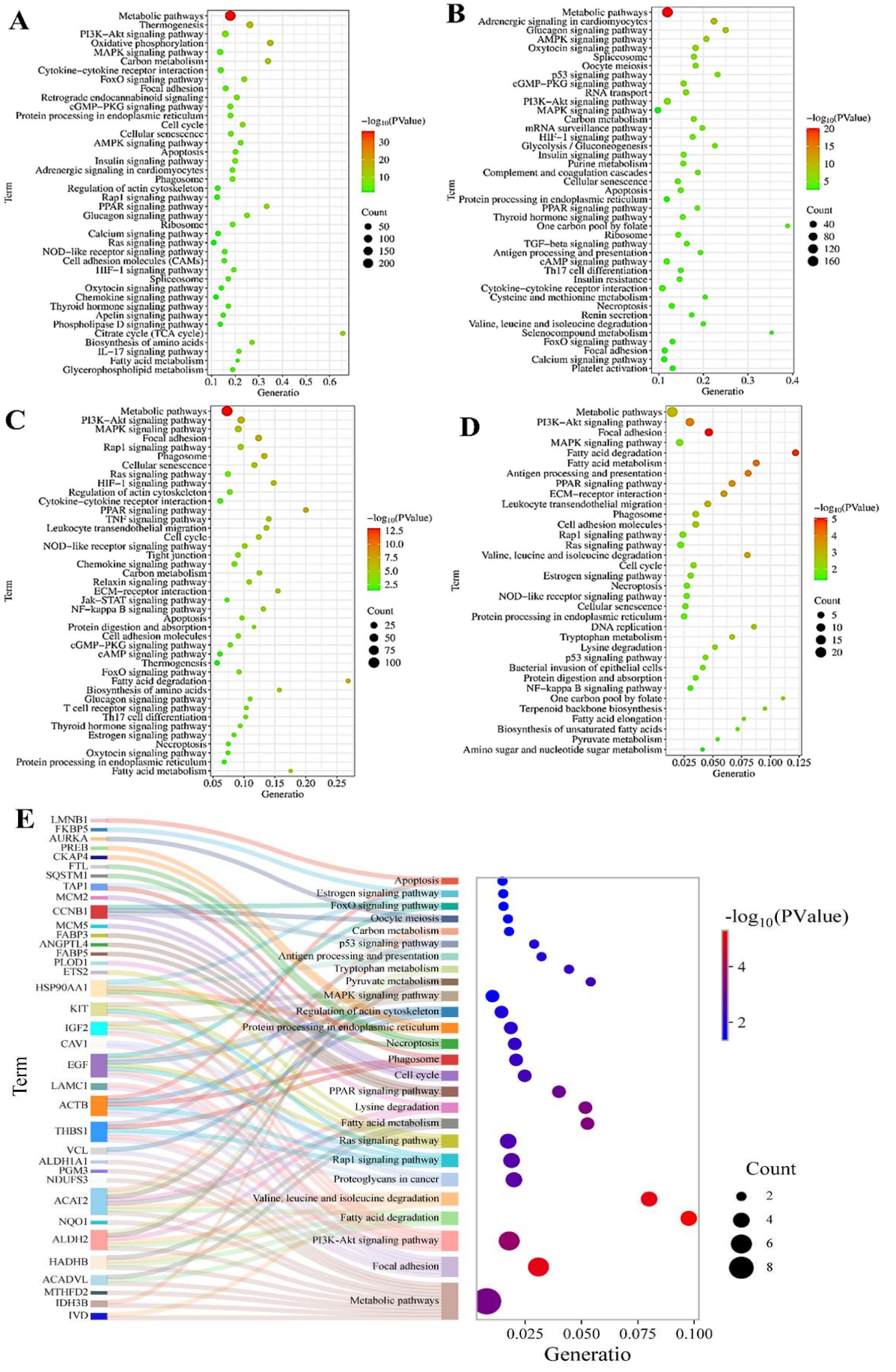
A
Metabolic pathways
Thermogenesis
PI3K−Akt signaling pathway
Oxidative phosphorylation
MAPK signaling pathway
Carbon metabolism
Cytokine−cytokine receptor interaction
FoxO signaling pathway
Focal adhesion
Retrograde endocannabinoid signaling
cGMP−PKG signaling pathway
Protein processing in endoplasmic reticulum
Cell cycle
Cellular senescence
AMPK signaling pathway
Apoptosis
Insulin signaling pathway
Adrenergic signaling in cardiomyocytes
Phagosome
Regulation of actin cytoskeleton
Rap1 signaling pathway
PPAR signaling pathway
Glucagon signaling pathway
Ribosome
Calcium signaling pathway
Ras signaling pathway
NOD−like receptor signaling pathway
Cell adhesion molecules (CAMs)
HIF−1 signaling pathway
Spliceosome
Oxytocin signaling pathway
Chemokine signaling pathway
Thyroid hormone signaling pathway
Apelin signaling pathway
Phospholipase D signaling pathway
Citrate cycle (TCA cycle)
Biosynthesis of amino acids
IL−17 signaling pathway
Fatty acid metabolism
Glycerophospholipid metabolism
Term
Generatio
−log10(PValue)
Count
B
Metabolic pathways
Adrenergic signaling in cardiomyocytes
Glucagon signaling pathway
AMPK signaling pathway
Oxytocin signaling pathway
Spliceosome
Oocyte meiosis
p53 signaling pathway
cGMP−PKG signaling pathway
RNA transport
PI3K−Akt signaling pathway
MAPK signaling pathway
Carbon metabolism
mRNA surveillance pathway
HIF−1 signaling pathway
Glycolysis / Gluconeogenesis
Insulin signaling pathway
Purine metabolism
Complement and coagulation cascades
Cellular senescence
Apoptosis
Protein processing in endoplasmic reticulum
PPAR signaling pathway
Thyroid hormone signaling pathway
One carbon pool by folate
Ribosome
TGF−beta signaling pathway
Antigen processing and presentation
cAMP signaling pathway
Th17 cell differentiation
Insulin resistance
Cytokine−cytokine receptor interaction
Cysteine and methionine metabolism
Necroptosis
Renin secretion
Valine, leucine and isoleucine degradation
Selenocompound metabolism
FoxO signaling pathway
Focal adhesion
Calcium signaling pathway
Platelet activation
Term
Generatio
−log10(PValue)
Count
C
Metabolic pathways
PI3K−Akt signaling pathway
MAPK signaling pathway
Focal adhesion
Rap1 signaling pathway
Phagosome
Cellular senescence
Ras signaling pathway
HIF−1 signaling pathway
Regulation of actin cytoskeleton
Cytokine−cytokine receptor interaction
PPAR signaling pathway
TNF signaling pathway
Leukocyte transendothelial migration
Cell cycle
NOD−like receptor signaling pathway
Tight junction
Chemokine signaling pathway
Carbon metabolism
Relaxin signaling pathway
ECM−receptor interaction
Jak−STAT signaling pathway
NF−kappa B signaling pathway
Apoptosis
Protein digestion and absorption
Cell adhesion molecules
cGMP−PKG signaling pathway
cAMP signaling pathway
Thermogenesis
FoxO signaling pathway
Fatty acid degradation
Biosynthesis of amino acids
Glucagon signaling pathway
T cell receptor signaling pathway
Th17 cell differentiation
Thyroid hormone signaling pathway
Estrogen signaling pathway
Necroptosis
Oxytocin signaling pathway
Protein processing in endoplasmic reticulum
Fatty acid metabolism
Term
Generatio
−log10(PValue)
Count
D
Metabolic pathways
PI3K−Akt signaling pathway
Focal adhesion
MAPK signaling pathway
Fatty acid degradation
Fatty acid metabolism
Antigen processing and presentation
PPAR signaling pathway
ECM−receptor interaction
Leukocyte transendothelial migration
Phagosome
Cell adhesion molecules
Rap1 signaling pathway
Ras signaling pathway
Valine, leucine and isoleucine degradation
Cell cycle
Estrogen signaling pathway
Necroptosis
NOD−like receptor signaling pathway
Cellular senescence
Protein processing in endoplasmic reticulum
DNA replication
Tryptophan metabolism
Lysine degradation
p53 signaling pathway
Bacterial invasion of epithelial cells
Protein digestion and absorption
NF−kappa B signaling pathway
One carbon pool by folate
Terpenoid backbone biosynthesis
Fatty acid elongation
Biosynthesis of unsaturated fatty acids
Pyruvate metabolism
Amino sugar and nucleotide sugar metabolism
Term
Generatio
−log10(PValue)
Count
E
LMNB1
FKBP5
AURKA
PREB
CKAP4
FTL
SQSTM1
TAP1
MCM2
CCNB1
MCM5
FABP3
ANGPTL4
FABP5
PLOD1
ETS2
HSP90AA1
KIT
IGF2
CAV1
EGF
LAMC1
ACTB
THBS1
VCL
ALDH1A1
PGM3
NDUFS3
ACAT2
NQO1
ALDH2
HADHB
ACADVL
MTHFD2
IDH3B
IVD
Apoptosis
Estrogen signaling pathway
FoxO signaling pathway
Oocyte meiosis
Carbon metabolism
p53 signaling pathway
Antigen processing and presentation
Tryptophan metabolism
Pyruvate metabolism
MAPK signaling pathway
Regulation of actin cytoskeleton
Protein processing in endoplasmic reticulum
Necroptosis
Phagosome
Cell cycle
PPAR signaling pathway
Lysine degradation
Fatty acid metabolism
Ras signaling pathway
Rap1 signaling pathway
Proteoglycans in cancer
Valine, leucine and isoleucine degradation
Fatty acid degradation
PI3K-Akt signaling pathway
Focal adhesion
Metabolic pathways
Term
-log10(PValue)
Count
Generatio

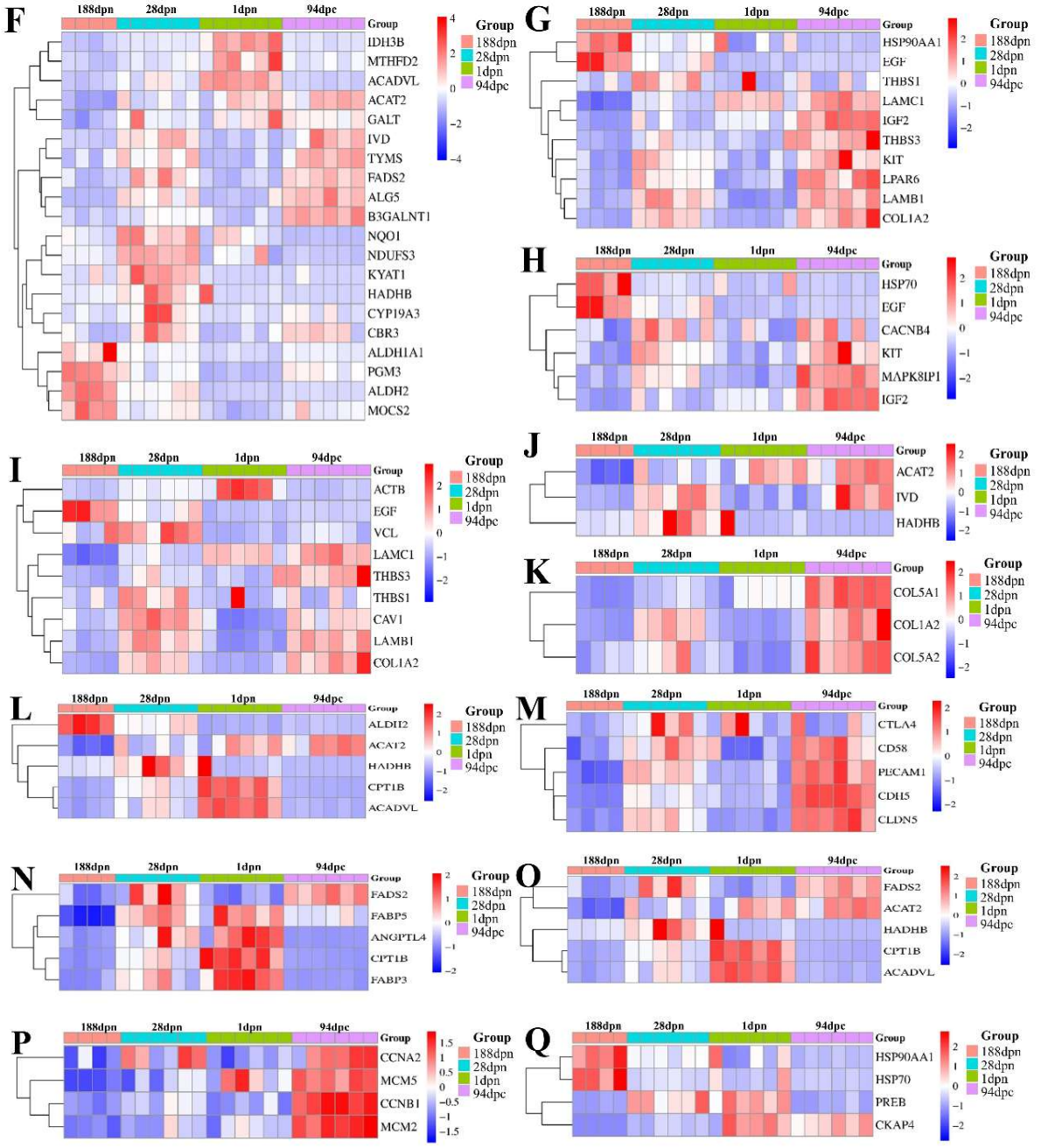

Fig. 3: KEGG functional enrichment for DEGs. (A-D) reveal KEGG enrichment for the DEGs identified in the comparison of 1dpn vs. 94dpc, 28 vs. 1dpn, and 188 vs. 28dpn, and the common DEGs in the three comparisons mentioned above. (E) denotes KEGG enrichment for the metabolic reprogramming-related DEGs. (F-Q) indicate the expression patterns of the overlapping DEGs in signaling pathways of metabolic pathways, PI3K-Akt, MAPK, focal adhesion, valine, leucine, and isoleucine degradation; protein processing in the endoplasmic reticulum; fatty acid degradation, cell adhesion molecules, PPAR, fatty acid metabolism, cell cycle, and protein processing in the endoplasmic reticulum, respectively.

Identification and functional characterization of hub genes: To systematically identify key regulatory elements governing hepatic development, we have employed a multi-algorithm approach (MCC, EPC, MNC, Closeness) via CytoHubba for hub gene prioritization (Fig. 8A). Cross-analysis of metabolic reprogramming-associated DEGs has revealed nine evolutionarily conserved hub genes: *VCL, EGF*, *HSP90AA1*, *CCNB1*, *CAV1*, *LMNB1*, *KXD1*, *ACADVL*, and *HSDL2* (Fig. 8A), indicating that they play important roles in the development of porcine liver. KEGG pathway enrichment analysis (Fig. 8B) shows that these hub genes participate in many important biological processes, such as focal adhesion, fatty acid degradation, actin cytoskeleton regulation, PI3K-Akt, fatty acid metabolism, adherent junction, cell cycle, and Jak-STAT signaling pathways. Also, the functions of the hub genes can be seen in Table 9. For example, *CCNB1* binds to and activates *CDK1* to promote the transition from G2 to M phase of the cell cycle (Table 9). Ensured correct mitotic spindle formation and chromosome separation. EGF binds with the epidermal growth factor receptor and stimulates the proliferation and differentiation of epithelial cells. Activates MAPK and PI3K-Akt pathways for tissue repair and regeneration (Table 9).

Table 9: Hub metabolic reprogramming-associated genes in porcine liver development

Gene symbol	Full name	Function
LMNB1	Lamin B1	*LMNB1* encodes Lamin B1, a critical component of the nuclear lamina that maintains nuclear structure stability and chromatin organization. It facilitates mitotic spindle assembly during cell division and regulates DNA replication. Dysfunction in *LMNB1* is associated with cellular senescence, age-related disorders, and cancers due to disrupted nuclear integrity and abnormal gene expression.
KXD1	KxDL Motif Containing 1	*KXD1* produces a protein containing a conserved KxDL motif, which interacts with GTPases and autophagy-related proteins. It mediates vesicle transport between the endoplasmic reticulum and Golgi apparatus and may regulate autophagy-lysosome pathways.
ACADVL	Acyl-CoA dehydrogenase very long chain	*ACADVL* encodes a mitochondrial enzyme that initiates the beta-oxidation of very long-chain fatty acids (VLCFAs) by catalyzing their dehydrogenation. Defects in *ACADVL* cause VLCAD deficiency, a life-threatening metabolic disorder characterized by hypoglycemia, cardiomyopathy, and hepatic dysfunction due to impaired energy production.
HSDL2	Hydroxysteroid dehydrogenase like 2	*HSDL2* is a peroxisomal and endoplasmic reticulum-associated enzyme involved in lipid metabolism, potentially modulating cholesterol synthesis and fatty acid elongation. It shares structural similarity with steroid dehydrogenases and may influence cell proliferation. Overexpression of *HSDL2* correlates with tumor progression in certain cancers.
CAV1	Caveolin 1	*CAV1* is a structural component of caveolae, plasma membrane invaginations involved in endocytosis and lipid regulation. It modulates signaling pathways, including TGF-β and EGFR. *CAV1* also regulates nitric oxide production and has tumor-suppressive roles by inhibiting oncogenic kinases.
VCL	Vinculin	*VCL* links integrin receptors to the actin cytoskeleton at focal adhesions. It stabilizes cell-matrix interactions and transmits mechanical forces during cell adhesion and migration. Conformational changes in vinculin activate downstream signaling pathways that regulate tissue morphogenesis and wound healing.
CCNB1	Cyclin B1	*CCNB1* binds to and activates *CDK1* to drive the transition from G2 to M phase in the cell cycle. It ensures proper mitotic spindle assembly and chromosome segregation.
HSP90AA1	Heat shock protein 90 alpha family class A member 1	*HSP90AA1* is a molecular chaperone that stabilizes client proteins, including steroid receptors and kinases, under stress conditions.
EGF	Epidermal growth factor	*EGF* binds to the epidermal growth factor receptor to stimulate epithelial cell proliferation and differentiation. It activates MAPK and PI3K-Akt pathways, promoting tissue repair and regeneration.

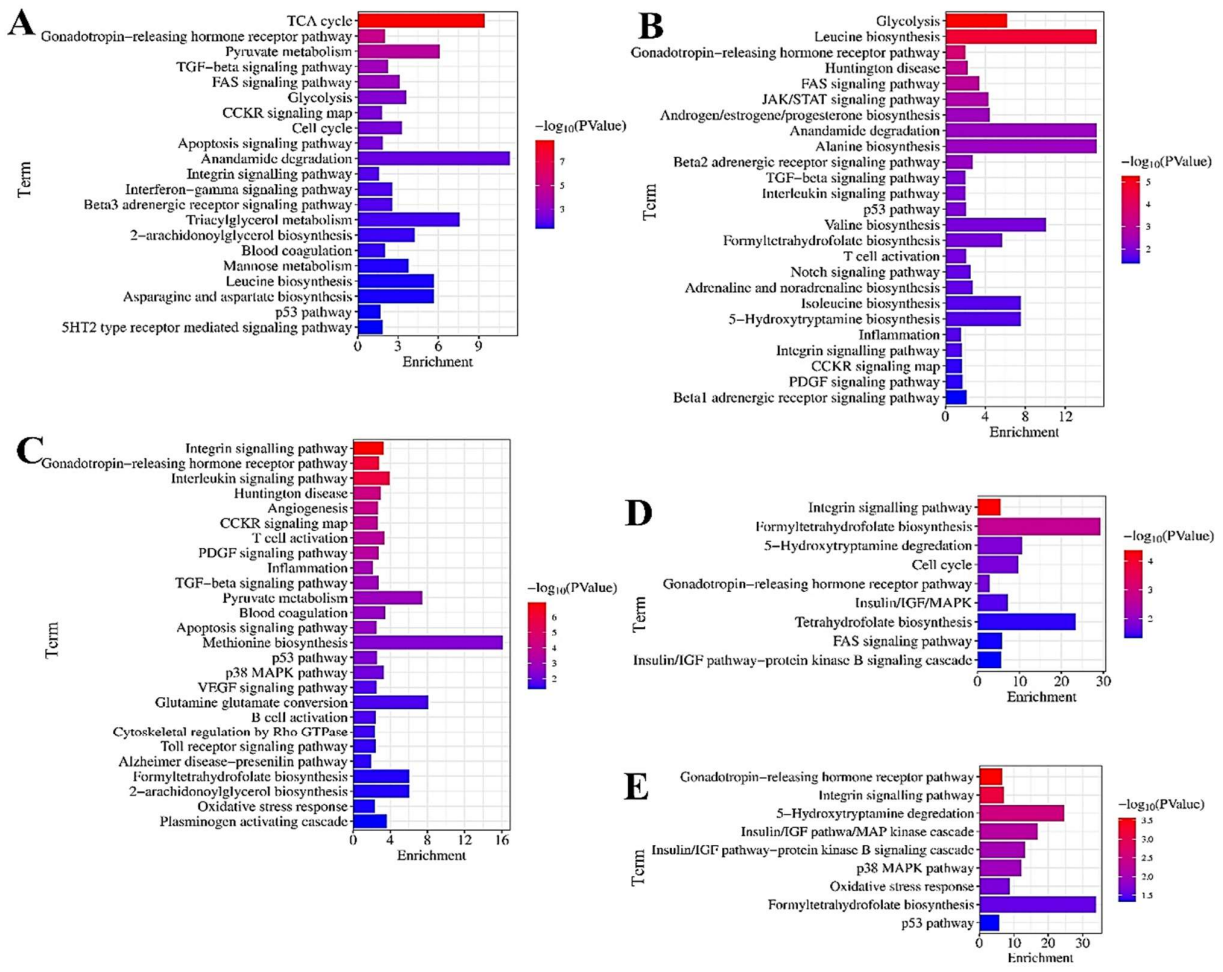

Fig. 4: Reactome pathway analysis of hepatic transcriptome dynamics. (A-D) represent Reactome enrichment for the DEGs identified in the comparison of 1dpn vs. 94dpc, 28 vs. 1dpn, and 188 vs. 28dpn, and the common DEGs in the three comparisons mentioned above. (E) confirms Reactome enrichment for the metabolic reprogramming-related DEGs

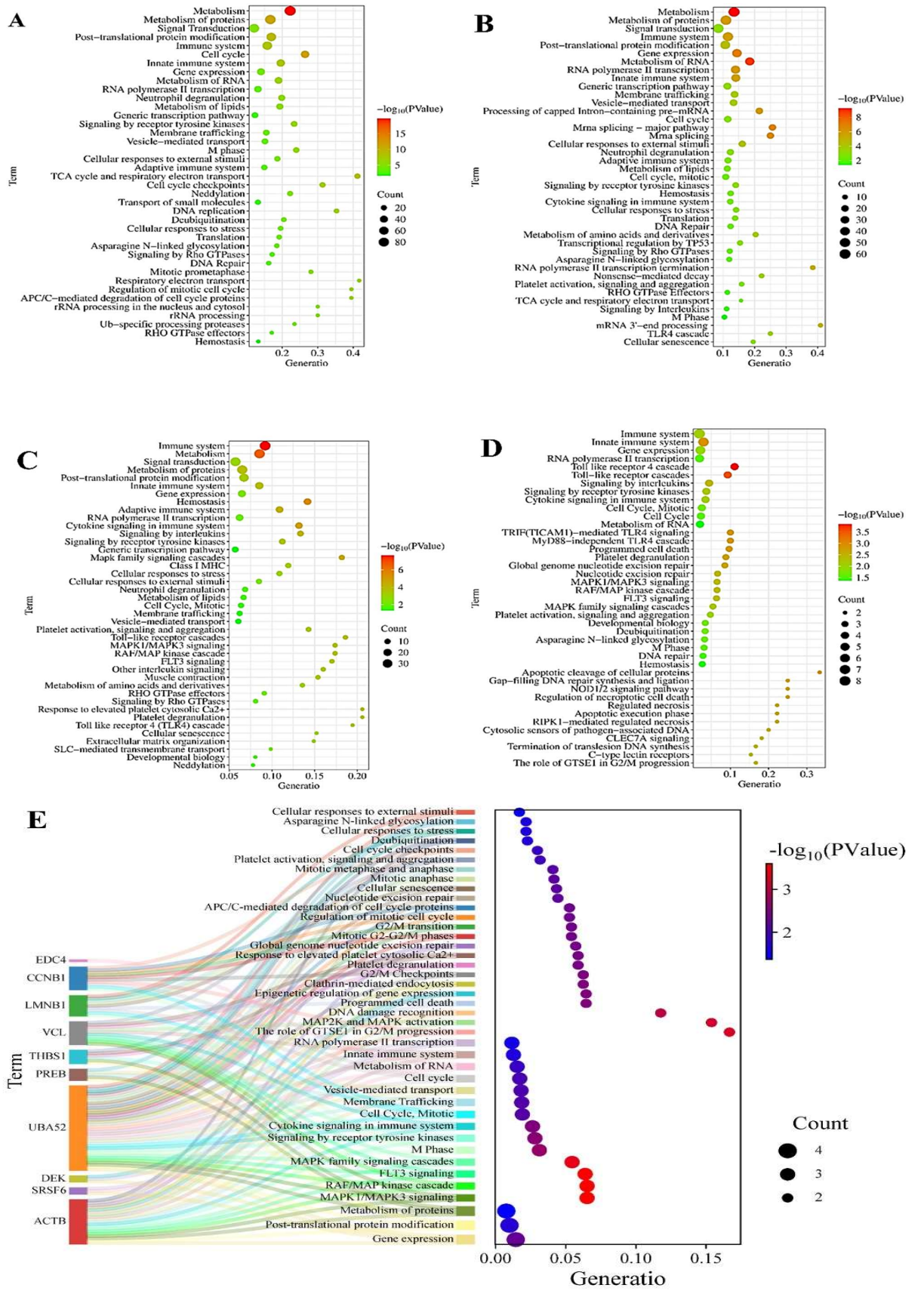

Fig. 5: PANTHER functional enrichment for the DEGs. (A-D) represent the PANTHER enrichment for the DEGs identified in the comparison of 1dpn vs. 94dpc, 28 vs. 1dpn, and 188 vs. 28dpn, and the common DEGs in the three comparisons mentioned above. (E) illustrates the PANTHER enrichment for the metabolic reprogramming-related DEGs.

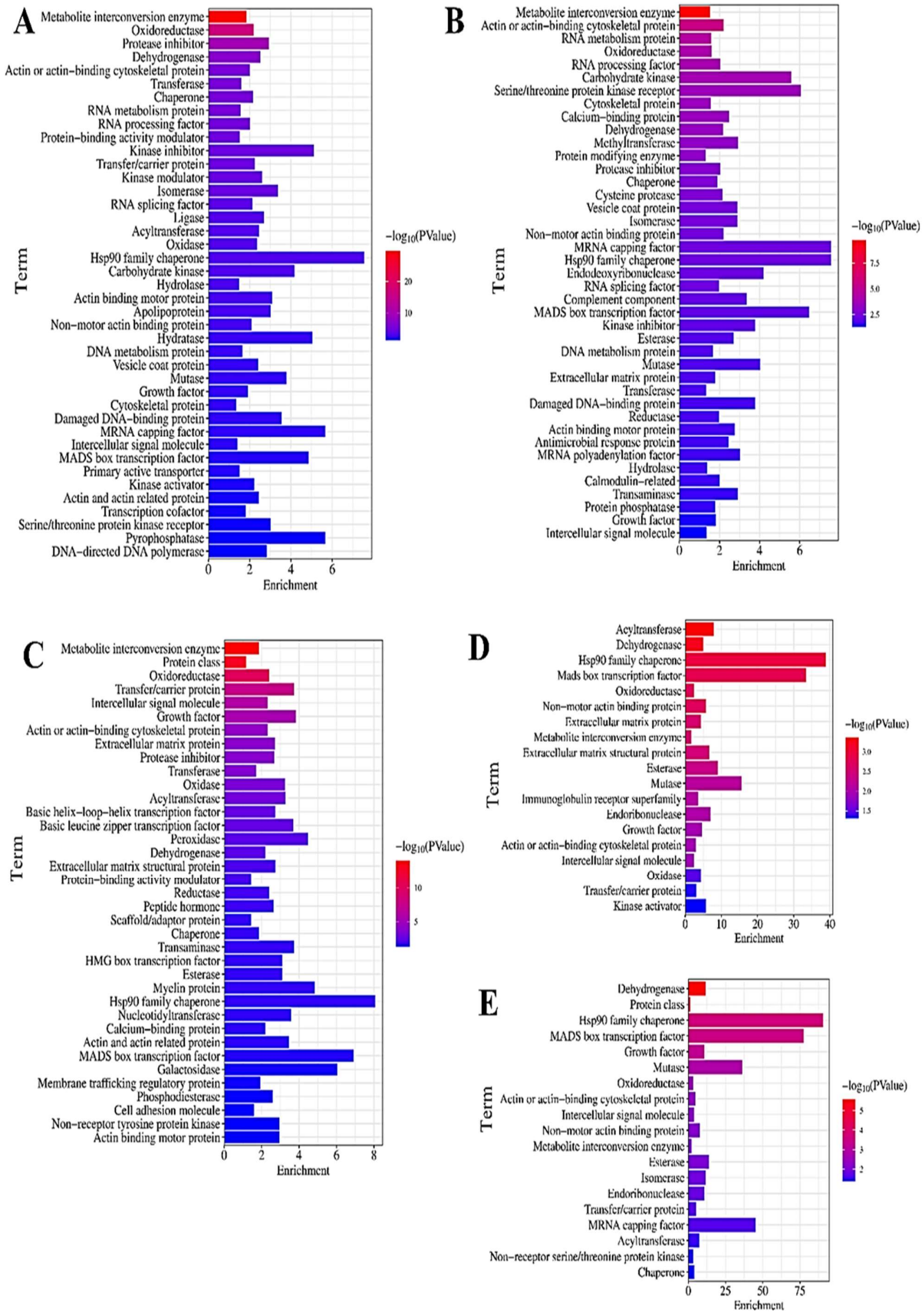

Fig. 6: Protein classification of the DEGs identified in pig livers. (A-D) represent the protein classification for the DEGs identified in the comparison of 1dpn vs. 94dpc, 28 vs. 1dpn, and 188 vs. 28dpn, and the common DEGs in the three comparisons mentioned above. (E) indicates the protein classification for metabolic reprogramming-related DEGs.

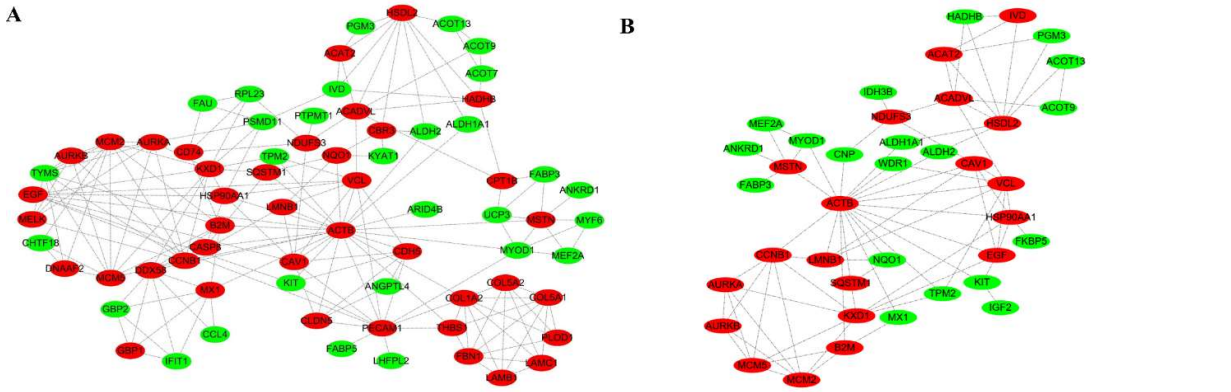

Fig. 7: PPI network of the DEGs in pig livers. (A) confirms PPI network constructed from commonly DEGs across the three comparisons; (B) indicates PPI network constructed from metabolic reprogramming related.

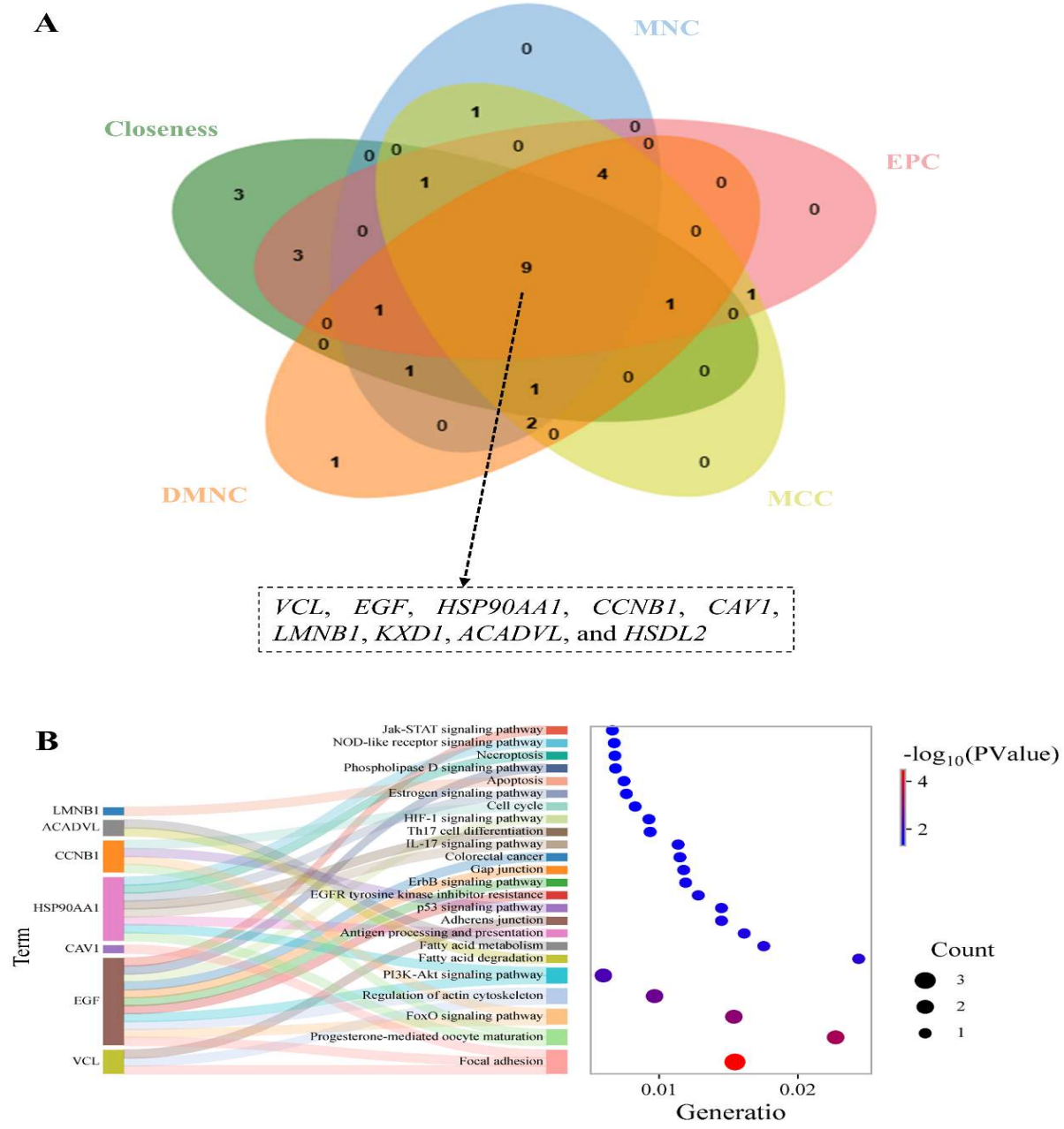

Fig. 8: Hub genes related to porcine liver development. (A) reveals hub genes related to pig liver development. (B) indicates KEGG enrichment for hub genes.

DISCUSSION

Metabolic reprogramming is a characteristic of liver growth that enables the organ to alter its functional and biosynthetic capacities throughout embryonic, perinatal, and postnatal stages of life (Rao *et al.*, 2023). During such changes, the hepatocytes change their way of using energy. This means switching from mainly relying on glycolysis for energy when cells were rapidly growing as embryos to using more oxidative phosphorylation and fat metabolism once they became adults (Zhang *et al.*, 2024).

In our study, we found that there are nine hub genes (including *LMNB1*, *KXD1*, and *ACADVL*) that are important for these metabolic changes, giving us some ideas about liver development in pigs. Liver metabolic flexibility has a close relationship with the development time. At 94dpc, hepatic primordia focus on fast cell division with glycolysis and nucleotide biosynthesis supporting them. Postnatally (1-188dpn): Metabolic needs change towards gluconeogenesis, fatty acid oxidation, and detoxification because they can eat food by themselves and experience physiological stress. DEGs decrease continuously from 1,939 (1 vs. 94dpc) to 880 (188 vs. 28dpn), which indicates a change from general transcriptional activation to specific regulation. Out of all the DEGs, there are 67 metabolic reprogramming related genes and their top 9 hubs that orchestrate the stage specific adaptation. Take *CCNB1* as an example; it controls the dynamics of the mitotic spindle and the proliferation and hypertrophy of hepatocytes (Alfonso-Pérez *et al.*, 2019; Tian *et al*., 2022), and *ACADVL* promotes postnatal lipid metabolism (Weber *et al.*, 2017). These hubs link external information to internal metabolic changes. Control of the cell cycle, structuring, and using substrates are some of the activities that come with modifying how the liver handles food.

Three hub genes (*LMNB1*, *CCNB1,* and *VCL*) indicate that mitotic control, cytoskeletal behavior, cell cycle progression, and metabolism are all connected (Prifti *et al.*, 2025; Nonnis *et al.*, 2025; Pendleton *et al.*, 2025). *LMNB1* makes lamin B1, which keeps the nuclear envelope stable as hepatoblasts grow (Pennarun *et al.*, 2021). It switches off immediately after birth (from 28dpn to 188dpn), which results in less mitosis occurring, allowing hepatocytes to exit the cell cycle and specialize into different types of cells. And the reduction of C*CNB1* (Cyclin B1) expression in hepatocytes during the embryonic stage (94dpc to 1dpn) also restrains development due to G2/M phase blockage (Wang *et al.*, 2014), yet it could facilitate differentiation via the cell cycle exit mechanism. This sort of regulation matches the requirement for area and time coordination at the start of the embryo's liver growth. *VCL* (vinculin), a focal adhesion protein, connects outside matrix interactions to inside metabolic signaling (Mansouri et al., 2023). It appears during the postnatal period (1-28dpn) along with liver zonation, where hepatocytes acquire distinct metabolic tasks depending on their location (periportal gluconeogenesis vs pericentral lipogenesis). *VCL* can help activate the PI3K-Akt pathway induced by ECM, and this pathway is involved in glucose uptake and glycogen synthesis (Mansouri *et al.*, 2017; Chen *et al.*, 2025). In pigs, the increase of *VCL* postnatally might go hand-in-hand with ECM remodeling (collagen deposition) and metabolic specialization so that form and function can develop.

After birth, pig's liver must have powerful fat metabolism to deal with the fats in milk and plant foods. Three hubs (*ACADVL*, *HSDL2,* and *CAV1*) control such changes. *ACADVL* (acyl-CoA dehydrogenase very long chain) does the first step of mitochondrial β-oxidation (Zhang e*t al.*, 2025), which is needed for making energy in pigs. It goes up from 94dpc to 1dpn at the same time as the influx of lipids, so it can get rid of fatty acids properly. In humans, *ACADVL* mutations lead to metabolic crises, indicating that they play a non-redundant role in lipid homeostasis (de Paula *et al.*, 2017). HSDL2 (hydroxysteroid dehydrogenase-like 2), though less known, might affect steroid action and bile acid creation (Li *et al.*, 2023; Samson *et al.*, 2024). Co-expression with *ACADVL* shows that they work together to control lipid processing. Similarly, *CAV1* (caveolin-1), a lipid raft scaffold protein, controls cholesterol transport and lipoprotein release (Fu *et al.*, 2004). In neonatal pigs, *CAV1* induction (1 to 28dpn) probably aids in bile acid expulsion and plasma membrane stability as liver cells are developing quickly. Also noteworthy is that *CAV1* also activates the PI3K-Akt pathway, which could aid in keeping the equilibrium between anabolic and catabolic procedures throughout a metabolic change (Sharp & Bartke, 2005; Tang *et al.*, 2015). All these genes make sure that lipids are kept in check throughout the process of growing up. *ACADVL* deficiency leads to hepatic lipid accumulation akin to a pediatric metabolic disorder (de Paula Simino *et al.*, 2017).

HSP90AA1 acts as a chaperone, and *KXD1* serves as an ER regulator addressing proteostatic and oxidative problems during liver growth. *HSP90AA1* stabilizes client proteins involved in cell signaling (e.g., Akt) and steroid receptor activation (Hu *et al.*, 2025). It's always there from the time you're a tiny baby growing inside your mom until you grow up to be a big person (from 94 days past conception to 188 days after birth), so maybe it helps protect against the kind of trouble that happens when your body doesn't get enough oxygen right before or right after you're born, or when it has to clean out some extra stuff from its system. In pigs, *HSP90AA1* might protect hepatocyte function if their food changes, just like it does for mice with fatty livers (Bidooki *et al.*, 2023). *KXD1* (KxDL motif containing 1), less studied, controls ER-Golgi traffic and COPII vesicle formation. It is a part of the maturation of the secretory pathway that is needed for making lysosome-related organelles (Yang *et al.*, 2012). These hubs show how stress adaptation connects with changing metabolism. *HSP90AA1* inhibition makes hepatocytes more sensitive to oxidative damage.

But there are two limitations. Firstly, without experimental verification such as qPCR and IHC, the spatiotemporal expression pattern of hub genes cannot be validated. Bioinformatics prioritization is good, but wet-lab experiments must confirm stage-specific protein location and activity. Secondly, what these genes do – especially those that aren't studied as much, such as *KXD1* and *HSDL2* – is still unknown. Take *KXD1,* for instance, does it directly influence the creation of COPII vesicles in hepatocytes, or does it collaborate with metabolic sensors such as mTORC1? Functional studies (CRISPR knockdown in porcine hepatocytes) should be carried out to determine their contribution to metabolic reprogramming. In the future, we could also explore the epigenetic and post-translational regulation of metabolic

reprogramming-related genes and how they interact with immune cells during liver development. Single-cell RNA sequencing might be able to be used here to solve the problem of cellular diversity and figure out if hub genes act on hepatocytes, Kupffer cells, or stellate cells.

Conclusions: This study shows that metabolism changes as the pig's liver develops by using all the info on how the liver is changing at different times. The number of DEGs drops from 1,939 to 880 along with the growth stage, showing a rise in transcription specialization. Out of the 182 conserved DEGs, we found 67 metabolic reprogramming related genes, most of which were associated with the development process and metabolic pathways. Network analysis identified nine hub genes (including *LMNB1*, *KXD1*, *ACADVL*, and *HSP90AA1*); *LMNB1* and *CAV1* were important regulators of hepatic differentiation and metabolic adaptation.

Funding: This study was supported by the Open Project of State Key Laboratory of Animal Biotech Breeding (No. 2024SKLAB6-10), the Open Project of State Key Laboratory of Tea Plant Biology and Utilization (No. SKLTOF20230121), and the Open Project of Longyan University & Fujian Provincial Key Laboratory for Prevention and Control of Animal Infectious Diseases and Biotechnology (No. ZDSYS2025003).

Data availability: The data in this study can be found in the current version of the manuscript and the supplementary material.

Authors contribution: Conceptualization: BY, Investigation and methodology: BZ, Supervision: BZ, Writing – original draft: BY, Writing – review & editing: BY.

Competing interests: Authors have declared that no competing interests exist.

REFERENCES

Alfonso-Pérez T, Hayward D, Holder J, *et al*., 2019. MAD1-dependent recruitment of CDK1-CCNB1 to kinetochores promotes spindle checkpoint signaling. Journal of Cell Biology 218:1108-1117.

Bidooki SH, Sanchez-Marco J, Martínez-Beamonte R, *et al*., 2023. Endoplasmic reticulum protein TXNDC5 interacts with PRDX6 and HSPA9 to regulate glutathione metabolism and lipid peroxidation in the hepatic AML12 cell line. International Journal of Molecular Sciences 24:17131.

Chen HJ, Liu PX, Pan X, *et al*., 2025. Downregulation of collagen IV deposition and ITGB1-FAK signaling pathway to inhibit adipogenesis:A new mechanism for swertiamarin in treating type 2 diabetes mellitus. International Journal of Biological Macromolecules 299:140048.

Cox AG, Hwang KL, Brown KK, *et al*., 2016. Yap reprograms glutamine metabolism to increase nucleotide biosynthesis and enable liver growth. Nature Cell Biology 18:886-896.

de Paula Simino LA, de Fante T, Fontana MF, *et al*., 2017. Lipid overload during gestation and lactation can independently alter lipid homeostasis in offspring and promote metabolic impairment after new challenge to high-fat diet. Nutrition & Metabolism 14:16.

Fu Y, Hoang A, Escher G, *et al*., 2004. Expression of caveolin-1 enhances cholesterol efflux in hepatic cells. Journal of Biological Chemistry 279:14140-14146.

Hu CW, Li ZY, Zhu K, *et al*., 2025. Exploring the effectiveness and potential pharmacological mechanism of minocycline for spinal cord injury through meta-analysis and network pharmacology. Current Neuropharmacology 23:1060-1080.

Kawai S, Enzan H, Hayashi Y, *et al*., 2003. Vinculin: A new marker for quiescent and activated hepatic stellate cells in human and rat liver. Virchows Archiv 443:78-86.

Khristi V, Ratri A, Ghosh S, *et al*., 2019. Disruption of ESR1 alters the expression of genes regulating hepatic lipid and carbohydrate metabolism in male rats. Molecular and Cellular Endocrinology 490:47-56.

Kokkinakis DM, Liu XY and Neuner RD, 2005. Modulation of cell cycle and gene expression in pancreatic tumor cell lines by methionine deprivation (methionine stress): Implication for the Therapy of Pancreatic Adenocarcinoma. Molecular Cancer Therapeutics 4:1338-1348.

Li JJ, Hu C, Ye YY, *et al*., 2025. HDAC inhibitor MS275 reprograms metabolism to induce differentiation and suppress proliferation in hepatocellular carcinoma. Frontiers in Immunology 16:1623211.

Li Y, Cen CQ, Liu B, *et al*., 2022. Overexpression of circ PTK2 suppresses the progression of nonalcoholic fatty liver disease via the miR-200c/SIK2/PI3K/Akt axis. Kaohsiung Journal of Medical Sciences 38:869-878.

Li YP, Zhao H, Pang M, *et al*., 2023. Expression profile of hydroxysteroid dehydrogenase-like 2 in *polychaete perinereis aibuhitensis* in response to BPA. Life 13:10.

Ma APY, Yeung CLS, Tey SK, *et al*., 2021. Suppression of ACADM-mediated fatty acid oxidation promotes hepatocellular carcinoma via aberrant CAV1/SREBP1 signaling. Cancer Research 81:3679-3692.

Mansouri M, Imes WD, Roberts OS, *et al*., 2017. FTY720 ameliorates renal fibrosis by simultaneously affecting leucocyte recruitment and TGF- signaling in fibroblasts. Clinical and Experimental Immunology 190:68-78.

Mansouri M, Imes WD, Roberts OS, *et al*., 2023. Fabrication of oxygen-carrying microparticles functionalized with liver ECM-proteins to improve phenotypic three-dimensional *In vitro* liver assembly, function, and responses. Biotechnology and Bioengineering 120:3025-3038.

Nakagaki BN, Mafra K, de Carvalho É, *et al*., 2018. Immune and metabolic shifts during neonatal development reprogram liver identity and function. Journal of Hepatology 69:1294-1307.

Nonnis S, Maffioli E, Grana J, *et al*., 2025. Relation between proteome characterization and semen quality in Italian chicken breeds. PLOS One 20:e0333802.

Oster M, Murani E, Metges CC, *et al*., 2012. Transcriptional response of skeletal muscle to a low-protein gestation diet in porcine offspring accumulates in growth- and cell cycle-regulating pathways. Physiological Genomics 44:811-818.

Pendleton E, Abdallah K, Chandar N, *et al*., 2025. Reduction in vinculin levels with Rb1 loss is responsible for altered differentiation in preosteoblasts. Experimental Cell Research451:114690.

Pennarun G, Picotto J, Etourneaud L, *et al*., 2021. Increase in lamin B1 promotes telomere instability by disrupting the shelterin complex in human cells. Nucleic Acids Research 49:9886-9905.

Prifti DK, Lauzier A, Garand, C, *et al*., 2025. ARHGEF17/TEM4 regulates the cell cycle through control of G1 progression. Journal of Cell Biology 224:e202311194.

Qian H, Chao XJ, Williams J, *et al*., 2021. Autophagy in liver diseases: A review. Molecular Aspects of Medicine82:100973.

Rao L, Cai LP and Huang LS, 2023. Single-cell dynamics of liver development in postnatal pigs. Science Bulletin 68:2583-2597.

Ruggeri R, Bee G and Ollagnier C, 2025. Review: Intrauterine growth restriction, diagnosis and physiological characterization in pigs. Animal 19:101590.

Samson N, Bosoi CR, Roy C, *et al*., 2024. HSDL2 links nutritional cues to bile acid and cholesterol homeostasis. Science Advances 10:eadk9681.

Sharp ZD and Bartke A, 2005. Evidence for down-regulation of phosphoinositide 3-kinase/Akt/mammalian target of rapamycin (PI3K/Akt/mTOR)-dependent translation regulatory signaling pathways in ames dwarf mice. Journal of Gerontology Series A: Biological Sciences and Medical Sciences 60:293-300.

Shastak Y, Pelletier W., 2024. Exploring the role of riboflavin in swine well-being: a literature review. Porcine Health Management 10:46.

Slabber CF, Tchorz and JS, 2025. Starvation induces metabolic hepatocyte reprogramming. Nature Metabolism7:864-866.

Tang WQ, Feng XM, Zhang S, *et al*., 2015. Caveolin-1 confers resistance of hepatoma cells to anoikis by activating IGF-1 pathway. Cellular Physiology and Biochemistry36:1223-1236.

Tian JN, Wang RM, Yang X, *et al*., 2022. Pregnane X receptor promotes liver enlargement in mice through the spatial induction of hepatocyte

hypertrophy and proliferation. Chemico-Biological Interactions 67:110133.

Wang ZQ, Fan M, Candas D, *et al*., 2014. Cyclin B1/Cdk1 coordinates mitochondrial respiration for cell-cycle G2/M progression. Developmental Cell 29:217-232.

Weber C, Schäff CT, Kautzsch U, *et al*., 2017. Variable liver fat concentration as a proxy for body fat mobilization postpartum has minor effects on insulin-induced changes in hepatic gene expression related to energy metabolism in dairy cows. Journal of Dairy Science 100:1507-1520.

Yang B, Li WH, Wang X, *et al*., 2025. Zinc finger protein Zfp335 is required for T cell homeostatic proliferation through regulating Lmnb1. Cell & Bioscience 15:139.

Yang Q, He X, Yang L, *et al*., 2012. The BLOS1-interacting protein KXD1 is Involved in the biogenesis of lysosome-related organelles. Traffic 13:1160-1169.

Zhang SH, Dang YL, Zhang QF, *et al*., 2015. Tetra-primer amplification refractory mutation system PCR (T-ARMS-PCR) rapidly identified a critical missense mutation (P236T) of bovine ACADVL gene affecting growth traits. Gene 559:184-188.

Zhang SL, Liu LH, Li XY, *et al*., 2024. Transcriptomic and proteomic sequencing unveils the role of vitamin D and metabolic flux shifts in the induction of human hepatic organoids. Stem Cell Research & Therapy 15:478.

Zhang YH, Yang XW, Jia ZX, *et al*., 2020. Proteomics unravels emodin causes liver oxidative damage elicited by mitochondrial dysfunction. Frontiers in Pharmacology11:416.

Zhou CR, Pan XM, Huang L, *et al*., 2024. Fibroblast growth factor 21 ameliorates cholestatic liver injury via a hepatic FGFR4-JNK pathway. Biochimica et Biophysica Acta - Molecular Basis of Disease1870:166870.